



## DC-to-DC Design Guide

Serge Jaunay, Jess Brown

### INTRODUCTION

Manufacturers of electronic systems that require power conversion are faced with the need for higher-density dc-to-dc converters that perform more efficiently, within a smaller footprint, and at lower cost—despite increasing output loads. To meet these demands, Siliconix has combined advanced TrenchFET<sup>®</sup> and PWM-optimized process technologies, along with innovative new packages, to provide:

- lowest on-resistance for minimum power dissipation
- lowest gate charge for minimum switching losses
- dV/dt shoot-through immunity<sup>1</sup>
- improved thermal management.

Breakthroughs in thermal management for increasing power density are being achieved with Vishay Siliconix packaging technologies such as the PowerPAK™ (Si7000 Series), the thick leadframe D<sup>2</sup>PAK (SUM Series), and ChipFET™ (Si5000 Series).

- The PowerPAK SO-8 offers the steady-state thermal resistance of a DPAK in an SO-8 footprint.
- The PowerPAK 1212-8 is approximately half the size of a TSSOP-8 while decreasing the thermal resistance by an order of magnitude.
- The SUM Series reduces thermal resistance by 33% over standard D<sup>2</sup>PAK packaging.
- ChipFET is 40% smaller than a TSOP-6 package while offering lower on-resistance and lower thermal resistance. It should be noted that lower thermal resistance results in higher possible maximum current and power dissipation.

The complete array of Vishay Siliconix MOSFET-packaged products ranges from the D<sup>2</sup>PAK (SUM or SUB series), DPAK (SUD Series), and PowerPAK (Si7000 Series) types of packages to the LITTLE FOOT<sup>®</sup> packages. These small outline devices range from the SO-8 down to the tiniest MOSFET available - the LITTLE FOOT SC-89.

### BACKGROUND MATERIAL

#### Switching Characteristics

The basic characteristics of a MOSFET are key to understanding how these devices work in switchmode power supplies.

In reality the freewheel diode will have some form of reverse recovery effect (3a and b, Figure 2), and as a result, the current through the drain source of the MOSFET (Q1, Figure 1) will increase. To accommodate the extra drain-source current,  $V_{GS}$  must increase above the value necessary to

support the load current. The gate voltage keeps rising until the device is carrying the combined load and recovery current (period 3). Therefore, the recovery current of the freewheel diode adds to the load current seen by the controlling MOSFET (Q1). At the end of period 3a, the reverse recovery current falls, along with the gate-source voltage. This is because the diode has recovered. The recovery current in turn will decay to zero, resulting in the gate voltage reducing to the original value required to support the load current (period 3b). During this period, the freewheel diode starts to support voltage, and the  $V_{DS}$  voltage falls, and the Miller Plateau begins. As with the ideal-recovery diode explanation, this continues until the voltage falls to its on-state value (end of 3) and the gate-source voltage is unclamped and continues to the applied gate-voltage value.

Turn-off is effectively the reverse of turn-on, apart from that there is no limitation by the freewheeling diode (in this particular circuit). For turn-off the Miller Plateau indicates the start of the rise of the drain-source voltage, and the voltage of the Miller Plateau will represent the required  $V_{GS}$  to sustain the load current. The turn-off delay is the period from when the gate voltage falls from its on-state value to when it reaches the Miller Plateau value (i.e. load-current value).

A simple buck converter, shown in Figure 1, shows the behavior of the MOSFET during turn-on and turn-off when switching an inductive load. During these periods, a positive step input is applied to turn the device on, and a step transition, from positive to zero, is applied to turn the MOSFET off.

With a positive step-input voltage on the gate, the voltage across the gate-source of the MOSFET ( $V_{GS}$ ) ramps up according to the time constant formed by the gate resistance ( $R_G$ ) and input capacitance ( $C_{ISS}$ ), as shown in Figure 2a (period 1). Once  $V_{GS}$  reaches the threshold voltage ( $V_{th}$ ), the channel is turned on, and the current through the device starts to ramp up (period 2). At the end of period 2, there are two possible switching transients that  $V_{GS}$  could follow. In the first case, the freewheel diode (D1, Figure 1) is assumed to have an ideal reverse recovery, represented by the solid waveforms in Figure 2. Once the channel is supporting the full-load current, the voltage across the device can begin to decay (the end of point 2) because the diode is now able to support voltage. As the drain-source voltage falls, the gate-source voltage stays approximately constant. This phenomenon is called the "Miller Plateau," and it continues until the voltage

<sup>a)</sup> Specifically designed to prevent spurious turn-on during high rates of dV/dt

<sup>b)</sup> SUM is an improved D<sup>2</sup>PAK package, with lower  $r_{DS(on)}$  and thermal resistance

falls to its on-state value. At the end of period 3 (Figure 2), the gate-source voltage is unclamped and continues to the applied gate-voltage value. This additional gate voltage fully enhances the MOSFET channel and reduces the  $r_{DS(on)}$ .

In reality the freewheel diode will have some form of reverse recovery effect (3a and b, Figure 2), and as a result, the current through the drain source of the MOSFET (Q1, Figure 1) will increase. To accommodate the extra drain-source current,  $V_{GS}$  must increase above the value necessary to support the load current. The gate voltage keeps rising until the device is carrying the combined load and recovery current (period 3). Therefore, the recovery current of the freewheel diode adds to the load current seen by the controlling MOSFET (Q1). At the end of period 3a, the reverse recovery current falls, along with the gate-source voltage. This is because the diode has recovered. The recovery current in turn will decay to zero, resulting in the gate voltage reducing to the original value required to support the load current (period 3b). During this period, the freewheel diode starts to support voltage, and the  $V_{DS}$  voltage falls, and the Miller Plateau begins. As with the ideal-recovery diode explanation, this continues until the voltage falls to its on-state value (end of 3) and the gate-source voltage is unclamped and continues to the

applied gate-voltage value.

Turn-off is effectively the reverse of turn-on, apart from that there is no limitation by the freewheeling diode (in this particular circuit). For turn-off the Miller Plateau indicates the start of the rise of the drain-source voltage, and the voltage of the Miller Plateau will represent the required  $V_{GS}$  to sustain the load current. The turn-off delay is the period from when the gate voltage falls from its on-state value to when it reaches the Miller Plateau value (i.e. load-current value).

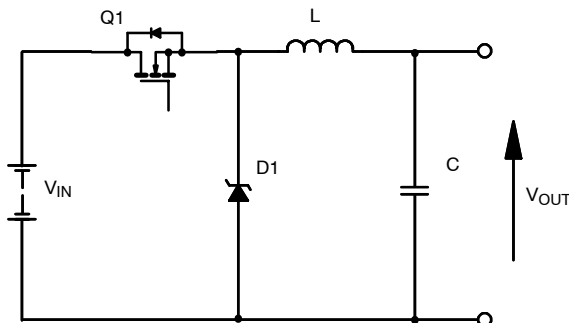


FIGURE 1. Typical circuit of a buck converter

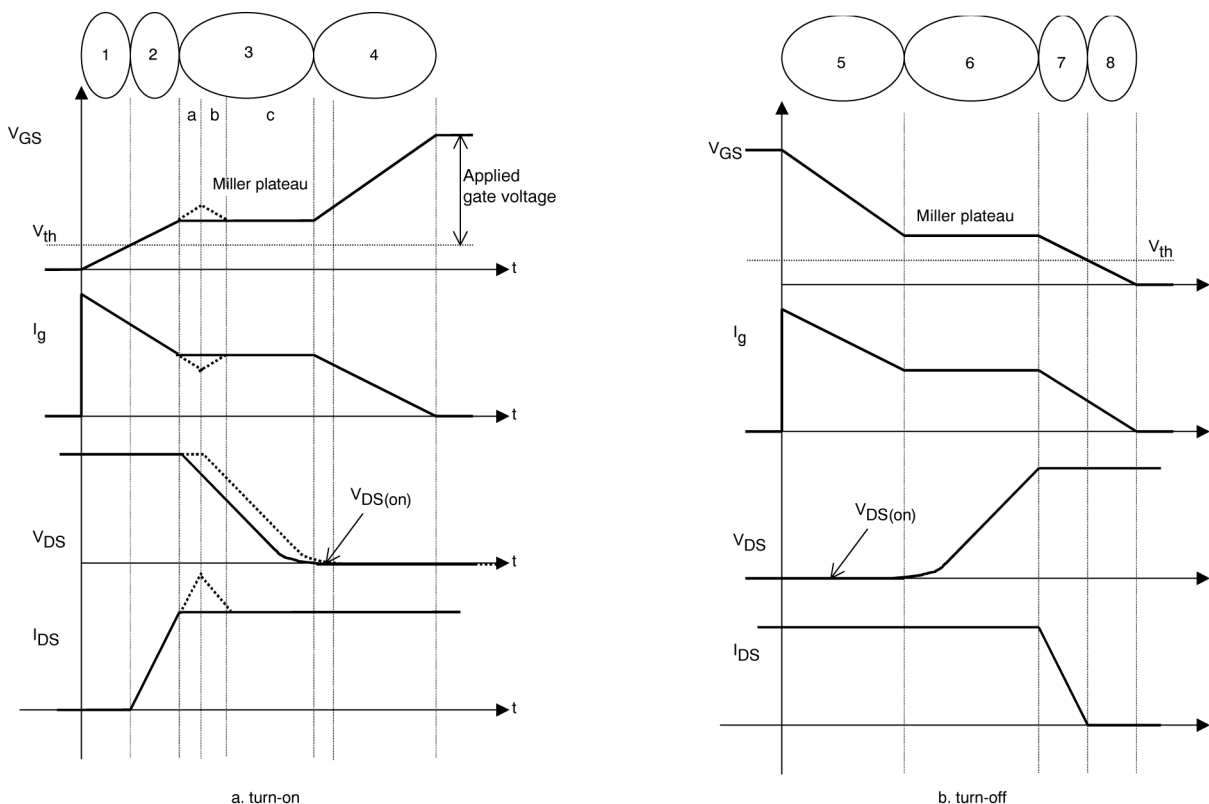


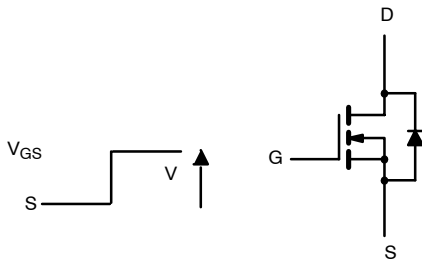
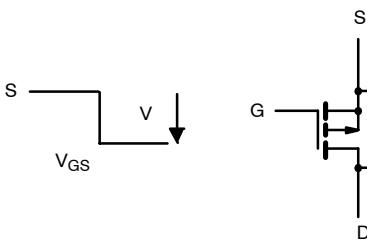
FIGURE 2. Switching waveforms for a typical MOSFET in a buck converter

Note: The solid line shows an idealized curve with no recovery of the anti-parallel diode. The dotted line shows the effect of

reverse recovery of the freewheel diode on the gate waveform and the corresponding switching waveforms.

**Driving MOSFETs: N- and P-Channel.**

There are two fundamental types of MOSFETs: n-channel and p-channel. An n-channel device needs a positive gate voltage with respect to the source voltage, whereas a p-channel MOSFET requires the gate voltage to be negative with respect to the source. Due to these criteria, each device sometimes appears to be geared for specific applications, such as p-channels for load switches and n-channels for low-side switches. In reality it is only the drive circuits that need to be different.


**FIGURE 3.** Schematic of an n-channel MOSFET

**FIGURE 4.** Schematic of a p-channel MOSFET

For the high-side switch portrayed in the buck converter of Figure 1, it would be possible to use either a p- or n-channel device; however, the operating conditions of the buck converter will determine which is to be used.

Again, consider the high-side MOSFET as shown in Figure 1. Once it is turned on, the source voltage will tend towards the drain voltage (minus the voltage across the device  $V_s \gg V_d$ ). Therefore, if the gate drive is generated from the input voltage ( $V_{in}$ ) as the MOSFET turns on,  $V_{GS}$  will reduce as the source pin ( $V_s$ ) goes to  $V_{in}$  ( $V_d$ ).

For an n-channel device, this means that the gate voltage must be higher than the drain voltage to maintain  $V_{GS}$  above the Miller Plateau voltage to ensure that the MOSFET stays fully on. To achieve this there are three common strategies or circuits:

- use an isolated supply with the 0 V referenced to the source voltage to ensure that the applied  $V_{GS}$  is the same as the voltage driving the gate;
- use a charge-pump circuit that generates a voltage higher than the dc-link voltage to drive the gate; or
- use a bootstrap circuit that again generates a voltage higher than the dc-link voltage, but which requires a switching circuit to charge up the bootstrap capacitor after the top device is turned off.

Another method is to use a p-channel device in situations in which the gate voltage does not need to be higher than the dc-link voltage. This is appropriate when the drain voltage of the MOSFET is less than 20 V because the gate signal can be derived directly from the input signal. With dc-link voltages  $>20$  V and with limitations of  $\gg 20$  V on maximum gate voltages, it is necessary to level-shift the applied gate voltage to ensure that the gate voltage does not exceed the maximum value. Therefore, with a dc-link voltage of 50 V, the applied gate voltage must be level-shifted to at least 30 V. It should also be noted that the performance characteristics of a p-channel generally are inferior to those of an n-channel due to the physical structure of the device.

For low-side devices, it is generally accepted that n-channel devices are used because the source connection of the MOSFET is connected to power ground. As such, the n-channel MOSFET only will require a positive signal referenced to power ground, whereas a p-channel device would require a negative signal to ground to keep the device turned on.

**Synchronous Rectification**

Improvements in efficiency can be made by replacing the rectifying diodes, or freewheel diodes, with MOSFETs. This is because the MOSFET has the capability to conduct current in both directions, and reductions in conduction loss can be achieved due to the  $I^2R$  losses of the MOSFET being lower than the  $IV$  losses associated with the diode. However, the circuit and load conditions will determine whether the increase in efficiency offsets the extra cost, and sometimes additional circuitry, demanded by synchronous MOSFETs.

It should be noted that the freewheel diode (D1, Figure 1), or rectifying diode, is still required to prevent both MOSFETs conducting at the same time – the necessity of dead time between Q1 and Q2 results in a short period of diode conduction – and causing shoot-through conditions. However, with the inclusion of a MOSFET, it is possible to use the inherent body diode, though this typically demonstrates performance inferior to that of an external Schottky diode. As a result, it is sometimes beneficial to use a Schottky diode as the anti-parallel diode bypassing the inherent body diode and resulting in an improvement of the conduction and recovery performance of the freewheel diode.

**NON-ISOLATED TOPOLOGIES**

**Non-isolated Buck Converter**

**Basic operation**

The buck (or step-down) converter, shown in Figure 5, is used to convert a positive dc voltage to a lower positive dc voltage. It can be a bi-directional converter, but for simplicity's sake, consider only the power flow from the higher voltage to the lower voltage.

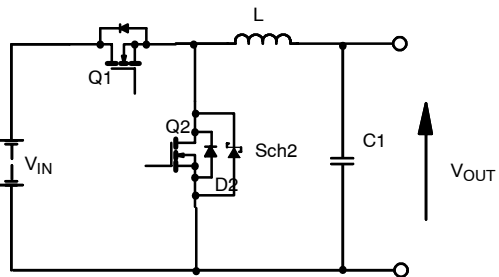


**FIGURE 5.** Basic circuit schematic for a buck converter

Note: Q2 is the MOSFET channel, D2 is the body diode of the MOSFET, and Sch2 is an external Schottky diode.

The input voltage has to be greater than the output voltage for energy to flow from the input through to the output.

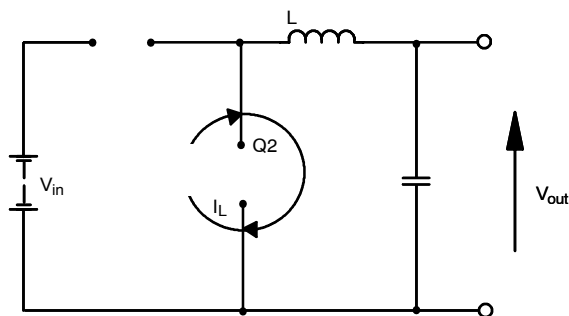


**FIGURE 6.** Turn-on of Q1

Figure 6 shows the turn-on of Q1. Because there is a positive voltage difference between  $V_{in}$  and  $V_{out}$ , there is a current build-up in the inductor according to:

$$\frac{di_L}{dt} = \frac{V_{in} - V_{out}}{L} \quad [1]$$

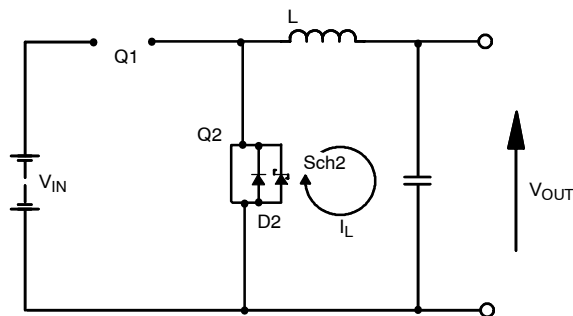


**FIGURE 7.** Turn-off of Q1

Once Q1 is turned off (Figure 7), the current flowing through the inductor cannot be reduced to zero instantaneously. Rather, the current requires a freewheel path, which will be Q2, D2, or Sch2, depending on the circuit topology. The current decays through the freewheel path according to:

$$\frac{di_L}{dt} = \frac{V_{out}}{L} \quad [2]$$

Table 1 shows the approximate voltage and current stresses for the buck converter based on continuous-conduction mode.

Table 1. Voltage and current stresses for the buck converter		
	Controlling Switch	Freewheel Element
Voltage (ideal)	$V_{in}$	$V_{in}$
Voltage (practical)	$V_{in} - I r_{DS(on)}$	$V_{in} + V_{out}$ or $V_{in} + I r_{DS(on)}$
Current pk (ideal)	$I_o$	$I_o$
Current pk (practical)	$I_o + \frac{\Delta I_o}{2}$	$I_o + \frac{\Delta I_o}{2}$
Current rms	$I_o \sqrt{\delta}$	$I_o \sqrt{1 - \delta}$

Figure 8 shows the idealized waveforms for the buck converter under continuous-current-mode operation.

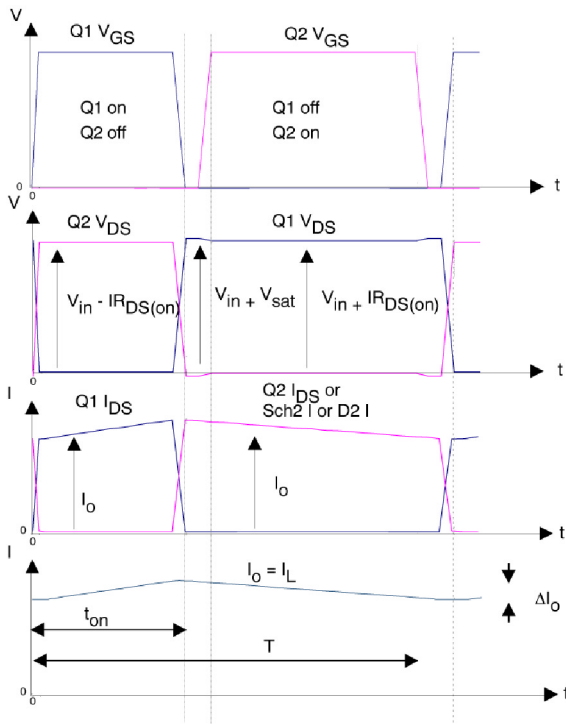


**FIGURE 8.** Current and voltage waveforms for the buck converter in constant-current operation

As shown in Figure 8, the input current will be the same as the current through the MOSFET Q1. This means that it will consist of a high-frequency current-square wave. If the input voltage is supplied by a battery, then the switched current will have a degrading effect on the battery life when compared with a continuous-current demand.

There are two modes of operation in a buck converter: continuous-current mode and discontinuous-current mode. In continuous mode the inductor current stays above zero for all load conditions, and the output voltage is directly related to duty cycle by the following equation:

$$V_{out} = V_{in} \frac{t_{on}}{T} = V_{in} \delta \quad [3]$$

In discontinuous-current operation, the inductor's minimum current reaches zero. The boundary condition is defined as:

$$I_o > \frac{V_{in}(1 - \delta)\delta T}{2L} \quad [4]$$

Therefore, to maintain continuous current, the load current ( $I_o$ ) must remain above a minimum value determined by the switching period ( $T$ ) and the inductance ( $L$ ).

During discontinuous-current mode, the output voltage is defined as:

$$V_{out} = \frac{V_{in}^2}{\frac{I_o^2 L}{\delta^2 T} + V_{in}} \quad [5]$$

Because the discontinuous-current mode of operation is dependent on load current, the buck converter normally is operated in continuous-current mode.

The high-side switch, Q1, can either be an n-channel or p-channel. If an n-channel MOSFET is used, then some form of charge pump or bootstrap is required to drive the gate of the MOSFET. If a p-channel MOSFET is used, it is sometimes necessary to use a level-shift circuit, depending on the dc-link voltage ( $V_{in}$ ).

### Synchronous rectification in a buck converter

The simplest method of providing the freewheel path is to use a diode (usually a Schottky diode) that has a low saturation voltage. Recent topologies implement synchronous rectification, where a MOSFET is used to conduct the current during the freewheel period. The MOSFET is turned on just after the freewheel diode goes into conduction, resulting in the current being transferred from the diode to the active region of the MOSFET, and it is turned off just before the controlling MOSFET, Q1, is turned on. The synchronous MOSFET is used because the  $I^2R$  power losses due to the  $r_{DS(on)}$  of the MOSFET will be less than the  $IV$  power losses associated with the saturation voltage of the diode.

However, even with synchronous rectification there is a small percentage of the switching time that the diode is in conduction, brought about by the necessity to ensure that both MOSFETs are not turned on at the same time. For that reason, in some topologies, a Schottky diode is used for this small period of diode conduction. Because there is little or no voltage present across the MOSFET during turn-off and turn-on, the switching losses of the synchronous MOSFET are reduced considerably.

### Losses in a buck converter<sup>1</sup>

The power loss of the MOSFET in the buck converter can be split into four categories: switching losses, on-state losses, off-state losses, and gate losses. However, the leakage currents in power semiconductor devices during the off state are several orders of magnitude smaller than the rated current and hence can be assumed to be negligible.

#### Conduction losses

The generic conduction losses can be equated to the product of the saturation voltage of the device ( $V_{DS(sat)}$ ) under consideration, the current ( $I$ ) through it, and the time the device is on ( $t_{on}$ ) of the switching waveform:

$$P_{con} = V_{ds(sat)} I t_{on} \quad [6]$$

The conduction voltage across a saturated power semiconductor junction consists of a constant component

Vishay Siliconix

( $V_{TO}$ ), plus a component that depends linearly upon current ( $k_{TO}$ ), as described by Equation 7.

$$V_{ds(sat)} = V_{TO} + k_{TO}I \quad [7]$$

Therefore, the conduction power loss of the switching device at a constant duty cycle operation is:

$$P_T = \frac{1}{T_c} \int_0^{t_{on}} V_{ds(sat)} I \quad [8]$$

where  $T_c$  is the period of the carrier frequency or:

$$P_{con} = \frac{(V_{TO} + k_{TO}I)It_{on}}{T_c} \quad [9]$$

Because a MOSFET is purely a resistive element, Equation 9 can be expressed as:

$$\begin{aligned} P_{con} &= \frac{k_{TO}I^2t_{on}}{T_c} = k_{TO}I^2\delta \quad [10] \\ &= r_{DS(on)}I^2\delta \end{aligned}$$

Likewise, the conduction power loss of the freewheeling diode is:

$$P_D = (V_{DO} + k_{DO}I)(1 - \delta)I \quad [11]$$

**Conduction losses with synchronous rectification**

With synchronous rectification there will be a time when either the body drain diode or external Schottky diode will be in conduction. This period can be approximated to the dead time ( $t_{deadtime}$ ). Hence, Equation 11 should be replaced by the following two equations for synchronous rectification.

$$P_{con} = r_{DS(on)}I^2(1 - \delta - t_{deadtime}f_{sw}) \quad [12]$$

$$P_D = (V_{DO} + k_{DO}I)(t_{deadtime}f_{sw})I \quad [13]$$

The values for the  $r_{DS(on)}$  should be taken at a realistic value by estimating the junction temperature of the device and using the normalized curve for the MOSFET. A typical graph is shown in Figure 9.

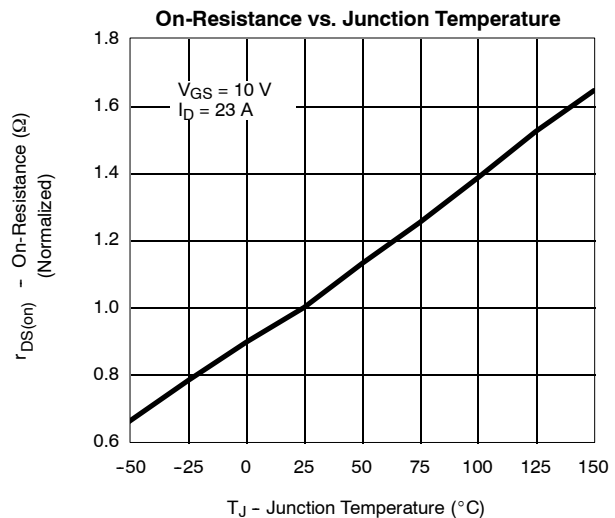


FIGURE 9. Normalized  $r_{DS(on)}$  versus temperature for a typical device

**Switching losses**

Switching losses are difficult to predict accurately and model because the parameters that make up switching transients vary greatly not only with temperature, but also with parasitic elements in the circuit. Furthermore, the gate-drive capability, gate-drive parasitics, and the operating conditions such as current and voltage influence the switching times, which are greatly dependent on individual circuit designs. Therefore, the following expressions for switching losses should be used to obtain an approximation of the performance of the device and should not be used as a definitive model.

To develop a loss model for the switching loss, consider an idealized switching waveform as shown in Figure 10. The switching losses can be separated into turn-on (from  $t_1$  to  $t_2$ ), turn-off (from  $t_5$  to  $t_6$ ), and recovery ( $t_2$  to  $t_4$ ) components.

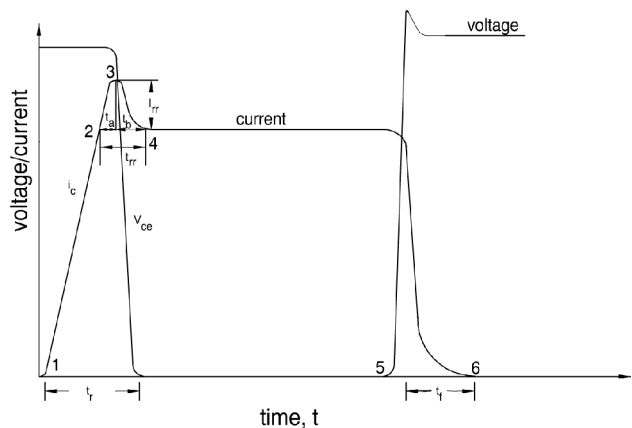


FIGURE 10. Idealized switching waveform for a MOSFET

Therefore, the energy dissipated during turn-on will be:

$$E_{on} = \int_0^{t_r} V_{in} \frac{I_o t}{t_r} dt \quad [14]$$

Hence:

$$E_{on} = \frac{1}{2} V_{in} t_r I_o \quad [15]$$

While the power can be found by:

$$P_{on} = \frac{1}{2} V_{in} t_r I_o f_s \quad [16]$$

The energy dissipated during turn-off is:

$$E_{off} = \frac{1}{2} V_{in} I_o t_f \quad [17]$$

And the corresponding power loss is:

$$P_{off} = \frac{1}{2} V_{in} I_o t_f f_s \quad [18]$$

The **recovery losses** due to the freewheeling diode occur from time  $t_2$  to  $t_4$  in Figure 10. At time  $t_2$ , the current in the switching device increases beyond the load current, owing to the stored charges in the freewheeling diode. At time  $t_3$ , a depletion region is formed in the freewheel diode. Then, the diode begins to support voltage, the stored charge disappears by recombination, and the collector voltage begins to fall. At time  $t_4$ , the recovery current can be assumed to be zero because it is within 10% of  $I_{rr}$ . The supply voltage,  $V_{in}$ , is completely supported by the switching device from  $t_2$  to the end of  $t_3$ , and hence the majority of the losses are generated in the switching device during this period. Assuming an

idealized near-triangular current waveform with  $I_{rr}$  being the peak recovery current, the switching device current may be expressed as the following function over the period  $t_a$ :

$$i = I_{rr} \frac{t}{t_a} + I_o \quad [19]$$

Integrating the instantaneous power over  $t_a$  ( $t_2$  to  $t_3$ ) to get the recovery loss gives:

$$E_{ra} = V_{in} t_a \left( \frac{I_{rr}}{2} + I_o \right) \quad [20]$$

From  $t_3$  to  $t_4$ , the losses are generated in both the freewheeling diode and the main device, and the voltage across the device reaches its on-state value at about the same time as the full recovery of the freewheel diode.

The instantaneous loss in the device is  $V_{ce} i_c$ , while the instantaneous loss in the diode is  $(V_{in} - V_{ce}) i_c$ . Hence, if the losses can be treated as one, the total power loss in the freewheel diode and device is the same as during  $t_a$ , which results in the total recovery loss being:

$$E_{rr} = V_{in} t_{rr} \left( \frac{I_{rr}}{2} + I_o \right) \quad [21]$$

And hence the power is:

$$P_{rr} = V_{in} t_{rr} \left( \frac{I_{rr}}{2} + I_o \right) f_s \quad [22]$$

A summary of a simple power-loss model for the buck and synchronous-buck converters described in the text above, is shown in Table 2.

<b>Table 2.</b> Summary of the generic loss equations for a buck converter		
	<b>Buck</b>	<b>Synchronous Buck</b>
Q1	$P_{con} = r_{DS(on)} I_o^2 \delta$ $P_{sw} = \frac{1}{2} V_{in} I_o (t_f + t_r) f_s$ $P_{gate} = Q_g V_g f_{sw}$	$P_{con} = r_{DS(on)} I_o^2 \delta$ $P_{sw} = \frac{1}{2} V_{in} I_o (t_f + t_r) f_s$ $P_{gate} = Q_g V_g f_{sw}$
Q2	—	$P_{con} = r_{DS(on)} I_o^2 (1 - \delta - \delta_{bbm})$ $P_{sw} \approx 0$ $P_{gate} = Q_g V_g f_{sw}$
D2 or Sch2	$P_{con} = V_{sat} I_o (1 - \delta)$	$P_{con} = V_{sat} I_o \delta_{bbm}$
Q1 & (D2 or Sch2)	$P_{rr} = V_{in} t_{rr} \left( \frac{I_{rr}}{2} + I_o \right) f_s$	$P_{rr} = V_{in} t_{rr} \left( \frac{I_{rr}}{2} + I_o \right) f_s$

The appropriate Vishay power ICs for non-isolated buck converters are shown in Appendix A.

Non-Isolated Boost Converter

Basic operation of a boost converter

The boost (or step-up) converter shown in Figure 11 is used to convert a positive dc voltage to a higher positive dc voltage. As with the buck converter, it can have a bidirectional power flow, but for simplicity's sake, consider only the power flow from the lower voltage to the higher voltage.

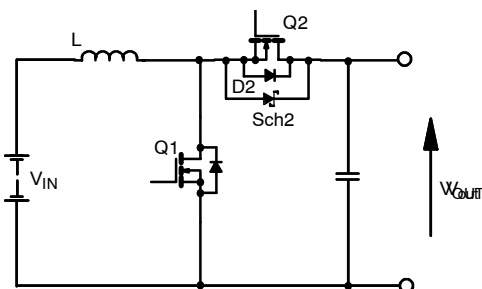


FIGURE 11. Basic circuit schematic for a boost converter

The input voltage must be less than the output voltage, otherwise the freewheel diode will be forward-biased, and uncontrolled power will flow.

Figure 12 shows the turn-on of Q1, which builds up the current in the inductor according to Equation 23. During this period, the output capacitor will have to support the load current.

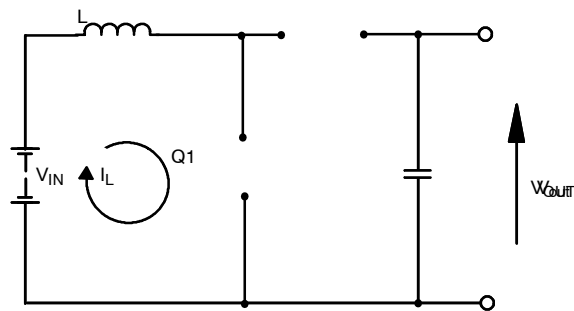


FIGURE 12. Turn-on of Q1

$$\frac{di_L}{dt} = \frac{V_{in}}{L} \quad [23]$$

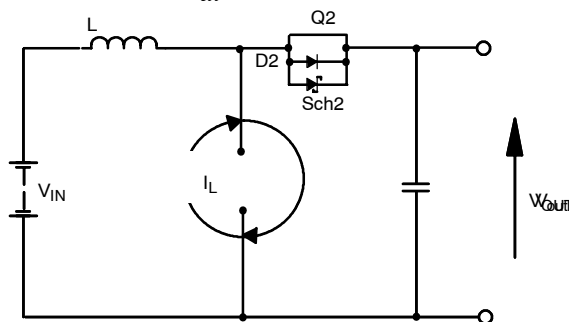
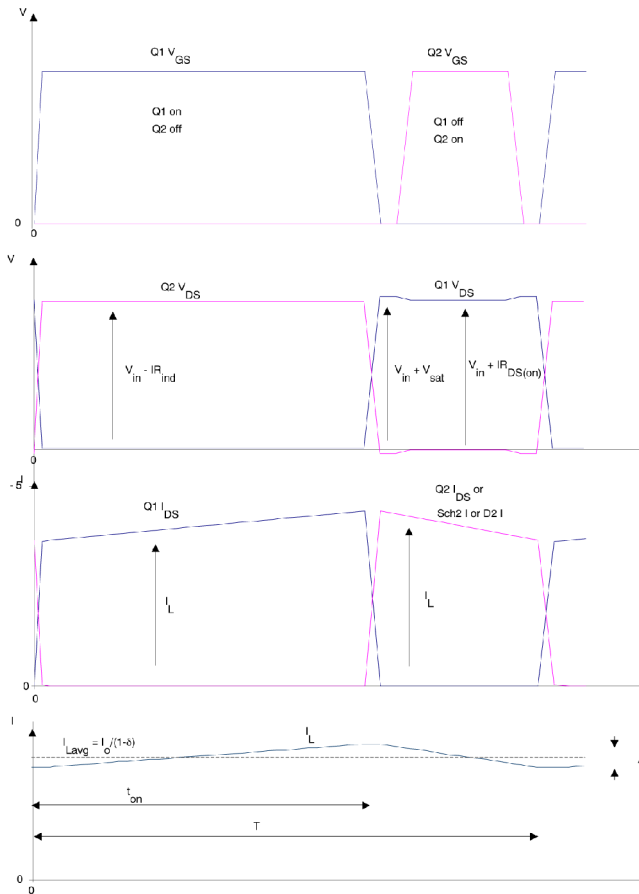


FIGURE 13. Turn-off of Q1

Once Q1 is turned off (Figure 13), the current flowing through the inductor is passed to the freewheel component, this being either the body drain diode, the Schottky diode, or the synchronous MOSFET, depending on the control strategy and the topology implemented. The current through the inductor decays according to Equation 24.

$$\frac{di_L}{dt} = \frac{V_{out} - V_{in}}{L} \quad [24]$$

Table 3. Voltage and current stresses for the boost converter		
	Controlling Switch	Freewheel Element
Voltage (ideal)	$V_{out}$	$V_{out}$
Voltage (practical)	$V_{out} - IR_{ind}$	$V_{out} + V_{dsat}$ or $V_{out} + Ir_{DS(on)}$
Current pk (ideal)	$\frac{I_o}{1 - \delta}$	$\frac{I_o}{1 - \delta}$
Current pk (practical)	$\frac{I_o}{1 - \delta} + \frac{\Delta I_o}{2}$	$\frac{I_o}{1 - \delta} + \frac{\Delta I_o}{2}$
Current rms	$\frac{I_o \sqrt{\delta}}{(1 - \delta)}$	$\frac{I_o}{\sqrt{1 - \delta}}$



**FIGURE 14.** Voltage and current-switching waveforms for a boost converter

The controlling MOSFET in this case is referenced to power ground, and therefore the simplest device to use is an n-channel. An advantage to using this topology is the fact that the input current consists of a continuous-current demand with a slight ripple, rather than a switched current.

Again, as with the buck converter, there are two modes of operation. In continuous-current mode, the output voltage is related to the duty cycle determined by:

$$V_{out} = V_{in} \frac{1}{1 - \delta} \quad [25]$$

The boundary between continuous and discontinuous operation is given by:

$$\bar{I}_o > \frac{V_{in}}{2L} T \delta (1 - \delta) \quad [26]$$

And for discontinuous operation the output voltage can be determined by:

$$V_{out} = V_{in} \left( \frac{V_{in} \delta^2 T}{2L \bar{I}_o} + 1 \right) \quad [27]$$

Once more, this is not an ideal solution, as the output voltage is dependent on load current.

### Synchronous rectification in a boost converters

As with the buck converter, there is a freewheel path required for the inductor current during the off-time of Q1. This current path can be provided with a Schottky diode, but with synchronous rectification the MOSFET provides the freewheel path. This reduces the conduction losses of the converter, as described in section 2.3.

### Losses in a boost converter Losses

The simple loss model for a boost converter is provided in Table 4. These equations are similar to those derived for the buck converter. However, in this case the inductor current is not the same as the load current, and as such, the rms current through the controlling MOSFET Q1 will be:

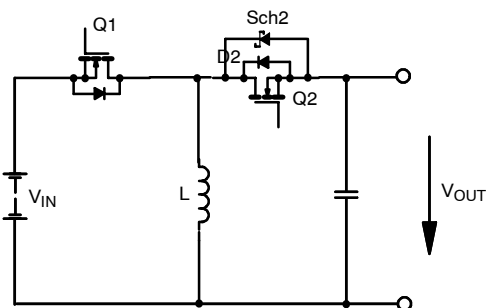
$$I_{rms} = \frac{I_o}{1 - \delta} \quad [28]$$

Table 4. Summary of the generic loss equations for a boost converter		
	Boost	Synchronous Boost
Q1	$P_{con} = r_{DS(ON)} \frac{I_o^2 \delta}{(1 - \delta)^2}$ $P_{sw} = \frac{1}{2} V_{in} \frac{I_o}{(1 - \delta)} (t_f + t_r) f_s$ $P_{gate} = Q_g V_g f_{sw}$	$P_{con} = r_{DS(ON)} \frac{I_o^2 \delta}{(1 - \delta)^2}$ $P_{sw} = \frac{1}{2} V_{in} \frac{I_o}{(1 - \delta)} (t_f + t_r) f_s$ $P_{gate} = Q_g V_g f_{sw}$
Q2	—	$P_{con} = r_{DS(on)} \frac{I_o^2}{(1 - \delta)^2} (1 - \delta - \delta_{bbm})$ $P_{sw} \approx 0 P_{gate} = Q_g V_g f_{sw}$
D2	$P_{con} = V_{sat} I_o$	$P_{con} = V_{dsat} \frac{I_o}{(1 - \delta)} \delta_{bbm}$
Q1 & D2	$P_{rr} = V_{in} t_{rr} \left( \frac{I_{rr}}{2} + \frac{I_o}{(1 - \delta)} \right) f_s$	$P_{rr} = V_{in} t_{rr} \left( \frac{I_{rr}}{2} + \frac{I_o}{(1 - \delta)} \right) f_s$

**Non-Isolated Buck-Boost Converter**

**Basic operation of a buck-boost converter**

The buck-boost, or inverting, converter is shown in Figure 15. As its name suggests, this converter either steps up or steps down the input voltage. The voltage output is negative with respect to the input voltage, due to the nature of the operation of the circuit.



**FIGURE 15.** Basic circuit schematic for the buck-boost converter

During turn-on of Q1, the current in the inductor will ramp up according to Equation 29.

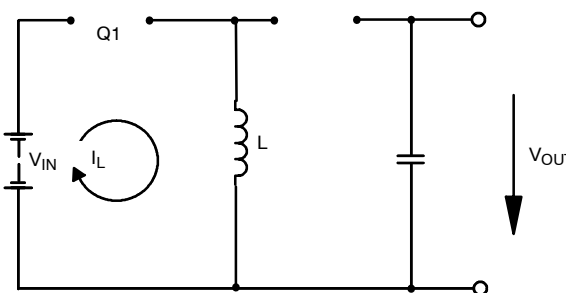


**FIGURE 16.** Turn-on of Q1

$$\frac{di_L}{dt} = \frac{V_{in}}{L} \quad [29]$$

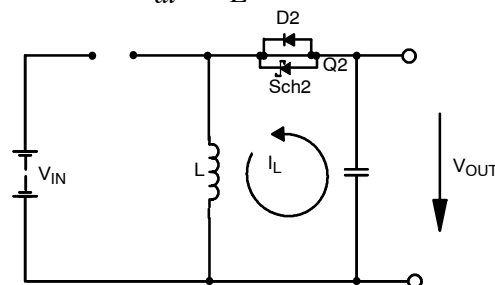


**FIGURE 17.** Turn-off of Q1

Once Q1 is turned off, the current in the inductor will decay according to Equation 30. However, the current in the inductor will force the output to be negative with respect to the input voltage.

$$\left| \frac{di_L}{dt} \right| = \frac{V_o}{L} \quad [30]$$

The voltage output for continuous operation is:

$$V_o = -V_{in} \frac{\delta}{1-\delta} \quad [31]$$

Therefore, for  $\delta < 0.5$  the magnitude of the output is smaller than the magnitude of the input, and for  $\delta > 0.5$  the magnitude of the output is greater than the magnitude of the input.

The boundary between continuous and discontinuous operation is given by:

$$\bar{I}_o > \frac{V_{in}}{2L} \delta T(1-\delta) \quad [32]$$

For discontinuous operation the output is:

$$V_o = V_{in} \frac{V_{in} T \delta^2}{2LI_o} \quad [33]$$

Which again is dependent on load current.

<b>Table 5.</b> Voltage and current stresses for the buck converter		
	<b>Controlling Switch</b>	<b>Freewheel Element</b>
Voltage (Ideal)	$V_{out} +  V_{in} $	$V_{out} +  V_{in} $
Voltage (practical)	$V_{out} - I r_{DS(on)}$ -	$V_{out} + V_{dsat}$ or $V_{out} + IR$
Current pk (ideal)	$\frac{I_o}{1-\delta}$	$\frac{I_o}{1-\delta}$
Current pk (practical)	$\frac{I_o}{1-\delta} + \Delta \frac{I_o}{2}$	$\frac{I_o}{1-\delta} + \Delta \frac{I_o}{2}$
Current rms	$\frac{I_o \sqrt{\delta}}{(1-\delta)}$	$\frac{I_o \sqrt{\delta}}{(1-\delta)}$

### Synchronous rectification in a buck-boost converter

As with the other non-isolated converters, there is a freewheel path required for the inductor current during the off-time of Q1. Synchronous rectification is provided by a MOSFET as shown in Figure 15. This has the advantage of reducing the

conduction losses dissipated in the converter. (See section 2.3.)

### Losses in a buck-boost converter

The generic losses in a buck-boost converter are given below in Table 6.

<b>Table 6.</b> Summary of the generic loss equations for a buck-boost converter		
	<b>Buck-Boost</b>	<b>Synchronous Buck-Boost</b>
Q1	$P_{con} = r_{DS(ON)} \frac{I_o^2 \delta}{(1-\delta)^2}$ $P_{sw} = \frac{1}{2} V_{in} \frac{I_o}{(1-\delta)} (t_f + t_r) f_s$ $P_{gate} = Q_g V_g f_{sw}$	$P_{con} = r_{DS(ON)} \frac{I_o^2 \delta}{(1-\delta)^2}$ $P_{sw} = \frac{1}{2} V_{in} \frac{I_o}{(1-\delta)} (t_f + t_r) f_s$ $P_{gate} = Q_g V_g f_{sw}$
Q2		$P_{con} = r_{DS(on)} \frac{I_o^2}{(1-\delta)^2} (1-\delta-\delta_{bbm})$ $P_{sw} \approx 0 P_{gate} = Q_g V_g f_{sw}$
Sch2 or D2	$P_{con} = V_{sat} I_o$	$P_{con} = V_{dsat} \frac{I_o}{(1-\delta)} \delta_{bbm}$
Q1 Sch2 or D2	$P_{rr} = V t_{rr} \left( \frac{I_{rr}}{2} + \frac{I_o}{(1-\delta)} \right) f_s$	$P_{rr} = V_{in} t_{rr} \left( \frac{I_{rr}}{2} + \frac{I_o}{1-\delta} \right) f_s$

## NON-ISOLATED CONVERTER APPLICATIONS

### Point of Load (POL) Converters

As required core voltages decrease to levels of 2.5 V and below, point of load converters are becoming more common in power-supply systems. These converters are placed at the point of use and are normally non-isolated because the isolation usually has been achieved by the front-end converter. There is a distributed voltage architecture - at present this is typically between 12 V and 8 V - and the point of load converters are generally synchronous-buck converters. However, there are trends for this voltage to be as low as 3.3 V. As these distributed voltages go lower, there is more need for boost converters and buck-boost converters.

POL converters enable designers to overcome the problems caused by the high peak-current demands and low-noise margins of the latest high-speed digital devices by situating individual, non-isolated, dc sources near their point of use. This helps to minimize voltage drops and noise pick-up/emission, and ensures tight regulation under dynamic load conditions.

## ISOLATED TOPOLOGIES

For some applications galvanic isolation is required to provide high-voltage isolation between the input voltage and output voltage. Therefore, isolated-converter topologies provide galvanic isolation and, due to the presence of a transformer, are able to convert practically any voltage level to another via the medium of the transformer. The transformer ratio is a key element, with the larger number-of-turns ratio providing the greater voltage change, but a badly designed transformer can lead to large inefficiencies in the converter.

One main trend in dc-to-dc converters is the increase in switching frequencies, which results in smaller magnetic components. However, without the introduction of resonant converters, the maximum switching frequency is highly dependent on the maximum available switching speed of the controlling or primary MOSFET. The higher the switching frequency, the higher the switching losses. If switched too quickly, this increased power dissipation could result in catastrophic failure of the MOSFET.

### Transformer Isolated Flyback Converter

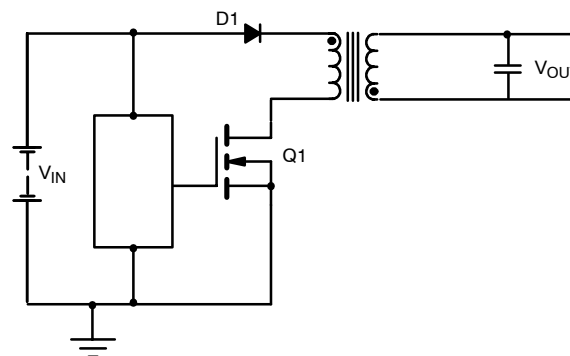


FIGURE 18. Schematic of an isolated flyback converter

The flyback transformer is the simplest of the isolated topologies, and usually it is used for low power levels in the region of 5 W to 100 W. These converters can provide either single or several outputs by the addition of secondary windings. The energy acquired by the transformer during the on-time of the primary MOSFET (Figure 18) is delivered to the output in the non-conducting period of the primary switch.

### Basic operation of a flyback converter

During the conduction period of the primary MOSFET, the current flows from the positive terminal (+) of the primary winding through the switch to ground. A voltage in the opposing direction is generated in the primary and secondary windings. Because the secondary winding is connected with reverse polarity, there can be no current flow to the output due to the blocking diode (D1).

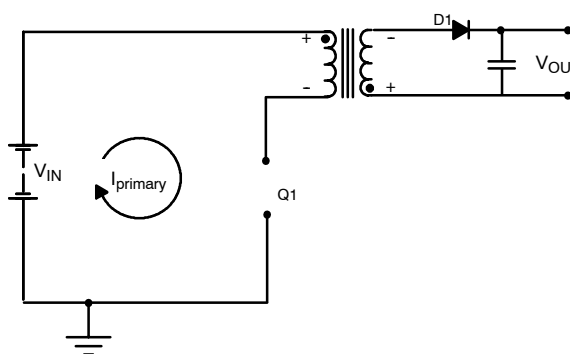
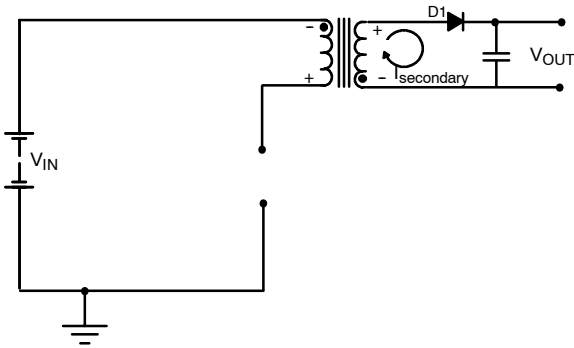


FIGURE 19. Schematic showing turn-on of Q1

When the primary MOSFET ceases to conduct, the induced voltage is reversed by the collapse of the magnetic field, and the output capacitor is charged through the diode (D1).



**FIGURE 20.** Schematic showing turn-off of Q1

In reality the isolation transformer (shown in Figure 18) is really a storage medium or coupled inductor. Energy is transferred to the output during the blocking or non-conducting period of the switching primary MOSFET. Energy is stored in the inductor when the transistor is turned on, and then it is delivered to the output when the transistor is turned off again.

In reality the isolation transformer (shown in Figure 18) is really a storage medium or coupled inductor. Energy is transferred to the output during the blocking, or non-conducting period of the switching primary MOSFET. Energy is stored in the inductor when the transistor is turned on, and then delivered to the output when the transistor is again turned off.

Flyback converters are more suitable than forward converters for relatively low power levels because of their lower circuit complexity resulting from the elimination of the output inductor and freewheel diode, which would be present in the secondary stage of a forward converter.

There are two modes of operation for a flyback converter: discontinuous and continuous. In discontinuous mode, all of the energy stored in the inductor is transferred to the output. This results in a smaller transformer and a feedback loop that is easier to stabilize.

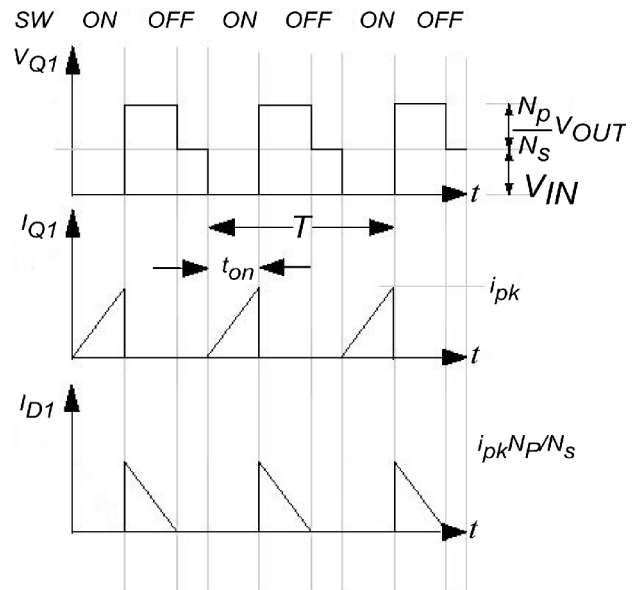


**FIGURE 21.** Current and voltage waveforms for a flyback converter in discontinuous mode

<b>Table 7. Voltage and current stresses for the flyback converter</b>		
	<b>Controlling switch</b>	<b>Freewheel element</b>
Voltage	$V_{in} + \frac{N_p}{N_s} V_{out}$	$V_{out} + \frac{V_{in} N_s}{N_p}$
Current rms	$\frac{I_{pk} \sqrt{\delta}}{\sqrt{3}}$	$\frac{I_{pk} N_p \sqrt{0.8 - \delta}}{N_s \sqrt{3}}$

Note: This assumes the converter is discontinuous for 20%.

In continuous mode only a portion of the stored energy is transferred to the output. This results in lower peak currents in output capacitors, but because it's more difficult to stabilize, it is not as common as the discontinuous flyback converter.

In continuous mode the output voltage depends on the duty cycle in an identical manner to that of a buck-boost converter, and it is:

$$V_o = V_{in} \frac{N_s}{N_p} \frac{\delta}{1 - \delta} \quad [34]$$

The average diode current also has a similar relationship as the buck-boost:

$$I_d = \frac{I_o}{1 - \delta} \quad [35]$$

And therefore, the average primary current is:

$$I_p = \frac{N_s}{N_p} \frac{I_o}{1 - \delta} \quad [36]$$

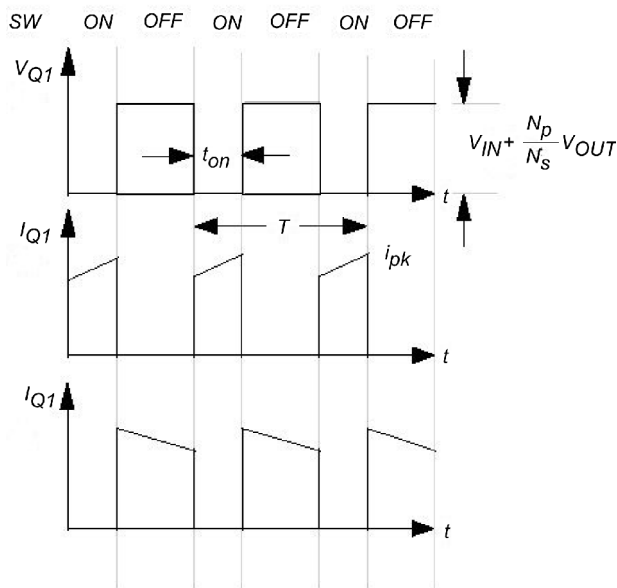


FIGURE 22. Current and voltage waveforms for a flyback converter in continuous mode

### Synchronous

Although synchronous rectification could be implemented in a flyback converter, usually it is not, due to the lower power levels and cost constraints associated with the flyback topology.

### Losses in a flyback converter

**Table 8.** Summary of the generic loss equations for a flyback converter

Flyback Discontinuous	
D1	$P_{con} = r_{DS(on)} \frac{I_{pk}^2}{3} \delta$ $P_{sw} = \frac{1}{2} \left( V_{in} + \frac{N_p}{N_s} V_{out} \right) \frac{I_{pk} \sqrt{\delta}}{\sqrt{3}} (t_f) f_s$ $P_{gate} = Q_g V_{g,sw} f_{sw}$
D1	$P_{com} = V_{dsat} \frac{N_p}{N_s} I_{pk} \frac{(0.8 - \delta)}{3}$
Flyback Continuous	
Q1	$P_{con} = r_{DS(on)} \left( \frac{N_s}{N_p} \right)^2 \frac{I_o^2 \delta}{(1 - \delta)^2}$ $P_{sw} = \frac{1}{2} \left( V_{in} + \frac{N_p}{N_s} V_{out} \right) \frac{N_s}{N_p} \frac{I_o \delta}{(1 - \delta)} f_s$ $P_{gate} = Q_g V_{g,sw} f_{sw}$
D1	$P_{con} = V_{dsat} I_o$

### Transformer Isolated Forward Converter

The forward converter is very similar to the step-down dc-to-dc converter, with the transformer providing galvanic isolation and not being used to store energy. For the topology investigated in this paper, a simple reset winding is included to reset the magnetizing current in the transformer to prevent core saturation<sup>2</sup>. The circuit used is a self-resonant reset circuit, which resets the magnetizing current and also recovers this magnetizing energy by charging it back to the input. This topology also allows for large ratios of input-to-output voltages.

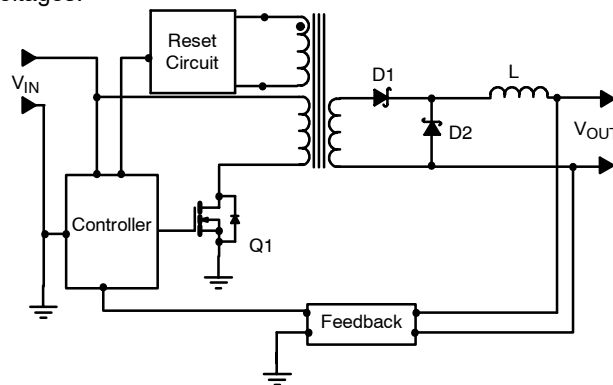


FIGURE 23. Schematic of an isolated forward converter

**Basic operation of a forward converter**

The forward converter does come in various configurations and is generally used for power levels from 10 W to 250 W. During the on-time, the power is transferred to the output via the diode D1. This is because D1 is forward-biased and D2 is reverse-biased, and the voltage across the output inductor can be determined by:

$$V_L = \frac{N_2}{N_1} V_{in} - V_{out} \quad [37]$$

During the off-time, the output inductor current circulates via D2 according to:

$$V_o = L \frac{di}{dt} \quad [38]$$

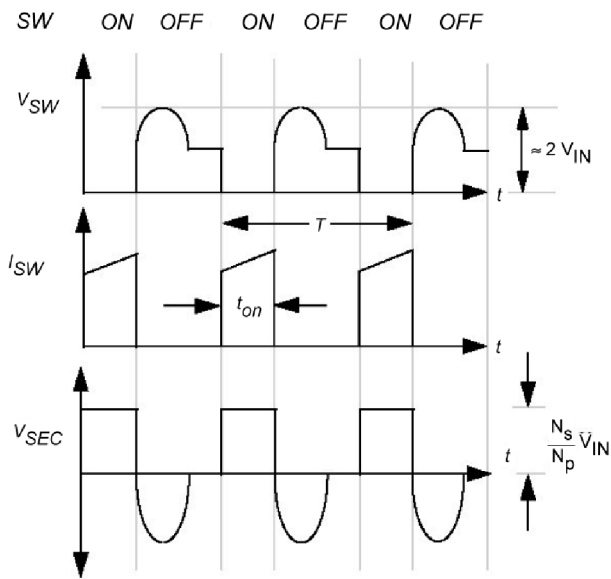


**FIGURE 24.** Current and voltage waveforms for a forward converter

**Synchronous rectification in a forward converter**

Synchronous rectification in a forward converter can be relatively easy to achieve, but there are several circuit configurations that can be used. One such circuit is the self-driven topology where the synchronous MOSFETs are driven directly from the secondary side of the transformer (Figure 25). One disadvantage of this circuit is the fact that the gate voltage for the synchronous MOSFETs is not constant. As a result, it is sometimes preferable to opt for a discrete driver solution as shown in Figure 26.

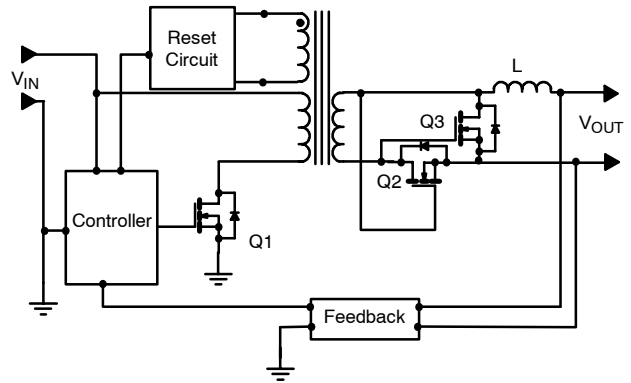


**FIGURE 25.** Self-driven synchronous rectification in a forward converter

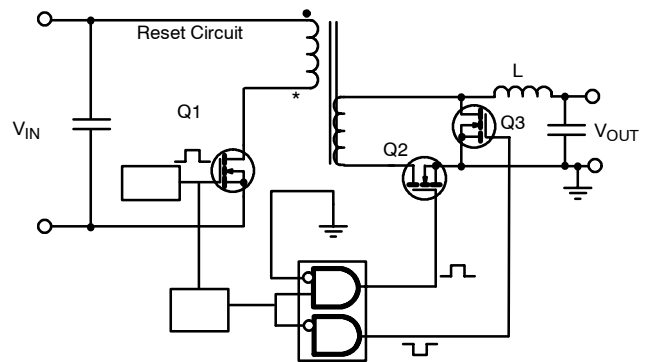


**FIGURE 26.** Synchronous rectification in a forward converter using a discrete driver

<b>Table 9.</b> Voltage and current stresses for the forward converter		
	<b>Controlling switch</b>	<b>Freewheel element</b>
Voltage	$2V_{in}$	$2V_{in} \frac{N_s}{N_p}$
Current pk	$I_o \frac{N_s}{N_p}$	$I_o$
Current rms	$\frac{I_o N_s \sqrt{\delta}}{N_p}$	$I_o \sqrt{\delta}$ for D1
		$I_o \sqrt{1 - \delta}$ for D2

**Losses in a forward converter.**

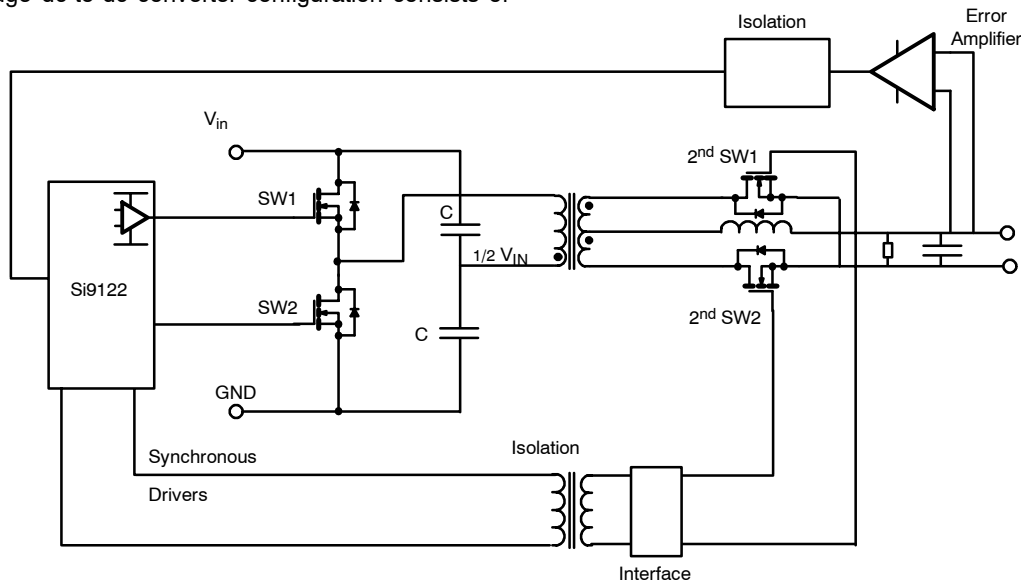
The simple loss model for the forward converter is shown in Table 6. This does not take into account synchronous rectification, as the losses will depend on which circuit topology is used. However, a simple approximation would be to substitute the saturation voltage of the diode with the IR product of the MOSFET.

Table 10. Summary of the generic loss equations for a forward converter	
Forward	
Q1	$P_{con} = r_{DS(on)} \left( \frac{N_s}{N_p} \right)^2 I_o^2 \delta$ $P_{sw} = \frac{1}{2} (t_f + t_r) V_{in} I_o \frac{N_s}{N_p} f_s$ $P_{gate} = Q_g V_g f_{sw}$
D1	$P_{con} = V_{dsat} I_o \delta$
D2	$P_{con} = V_{dsat} I_o (1 - \delta)$

two large, equal capacitors connected in series across the dc input, providing a constant potential of  $1/2 V_{in}$  at their junction, as shown in Figure 3. The MOSFET switches SW1 and SW2 are turned on alternatively and are subjected to a voltage stress equal to that of the input voltage. Due to the capacitors providing a mid-voltage point, the transformer sees a positive and negative voltage during switching. The result is twice the desired peak flux value of the core because the transformer core is operated in the first and third quadrant of the B-H loop and it experiences twice the flux excursion as a similar forward-converter core.

**Half-Bridge Isolated Converter**

The half-bridge dc-to-dc converter configuration consists of



**FIGURE 27.** Schematic of a half-bridge converter

**References and further reading**

1. "An assessment of the efficiencies of soft and hard switched inverters for applications in powered electric vehicles." A J Brown, PhD Thesis, December 2000, Department of Electronic and Electrical Engineering, The University of Sheffield, United Kingdom.
2. AN707. "Designing a High Frequency, Self-Resonant Reset Single Switch Forward Converter Using Si9118/Si9119 PWM/PSM."  
<http://www.vishay.com/document/70824/70824.pdf>
3. "Power Electronics, Converters, Applications and Design." Mohan, Undeland and Robbins, 2nd edition Wiley. ISBN 0-471-58408-8.



Alphanumeric Index															
Part Number	V <sub>DS</sub> (V)	V <sub>GS</sub> (V)	r <sub>DS(on)</sub> Ω				Q <sub>g</sub> (nC)		Q <sub>GS</sub> (nC)	Q <sub>GD</sub> (nC)	R <sub>g</sub> Typ (Ω)	V <sub>th</sub> (V)	I <sub>D</sub> (A)	P <sub>D</sub> (W)	Package
			V <sub>GS</sub> = 10V	V <sub>GS</sub> = 6V	V <sub>GS</sub> = 4.5V	V <sub>GS</sub> = 2.5V	V <sub>GS</sub> = 10V	V <sub>GS</sub> = 4.5V							
Si1302DL	30	20	0.4800		0.7000		0.9	0.5	0.2	0.1		1.0	0.6	0.3	SC70-3
Si1553DL	20	12			0.3850	0.6300		0.8	0.1	0.3		0.6	0.7	0.3	SC70-6
Si1553DL	-20	12			0.9950	1.8000		1.2	0.5	0.3		0.6	0.4	0.3	SC70-6
Si1900DL	30	20	0.4800		0.7000		0.9	0.5	0.2	0.1		1.0	0.6	0.3	SC70-6
Si2301DS	-20	8			0.1300	0.1900		5.8	0.9	1.7		0.5	2.3	1.3	SOT-23
Si2305DS	-8	8			0.0520	0.0710		10.0	2.0	2.0		0.5	3.5	1.3	SOT-23
Si2306DS	30	20	0.0570		0.0940		8.5	4.2	1.9	1.4		1.0	3.5	1.3	SOT-23
Si2308DS	60	20	0.1600		0.2200		4.8	2.3	0.8	1.0		1.5	2.0	1.3	SOT-23
Si2320DS	200	20	7.0000				1.1		0.3	0.4		2.0	0.3	1.3	SOT-23
Si2328DS	100	20	0.2500				3.3	2.0	0.5	1.5		2.0	1.5	1.3	SOT-23
Si3420DV	200	20	3.7000				2.2		0.7	1.0		2.0	0.5	2.1	TSOP-6
Si3422DV	200	20	5.0000				2.1		0.5	0.9		2.0	0.4	2.1	TSOP-6
Si3430DV	100	20	0.1700	0.1850	0.1850		5.5	3.0	1.5	1.4		2.0	2.4	2.0	TSOP-6
Si3443DV	-20	12			0.0650	0.1000		8.5	2.8	1.7		0.6	4.4	2.0	TSOP-6
Si3446DV	20	12			0.0450	0.0650		10.0	2.5	2.2		0.6	5.3	2.0	TSOP-6
Si3454ADV	30	20	0.0600		0.0850		9.0	4.5	2.5	1.5		1.0	4.5	2.0	TSOP-6
Si3454DV	30	20	0.0650		0.0950		8.0	3.5	1.8	1.3		1.0	4.2	2.0	TSOP-6
Si3456DV	30	20	0.0450		0.0650		12.0	5.7	2.8	1.6		1.0	5.1	2.0	TSOP-6
Si3458DV	60	20	0.1000		0.1300		8.0	3.9	4.0	2.0		1.0	3.2	2.0	TSOP-6
Si3460DV	20	8			0.0270	0.0320		13.5	2.3	2.2		0.5	6.8	2.0	TSOP-6
Si3552DV	-30	20	0.2000		0.3600		4.2	2.4	0.9	0.8		1.0	1.8	1.2	TSOP-6
Si3552DV	30	20	0.1050		0.1750		3.7	2.1	0.7	0.7		1.0	2.5	1.2	TSOP-6
Si3812DV	20	20			0.1250	0.2000		2.1	0.3	0.4		0.6	2.4	1.2	TSOP-6
Si3850DV	20	12			0.5000			0.8	0.3	0.2		0.6	1.2	1.3	TSOP-6
Si3850DV	-20	12			1.0000			1.1	0.5	0.2		0.6	0.9	1.3	TSOP-6
Si4300DY	30	20	0.0185		0.0330		15.0	8.7	2.3	4.2	1.9	0.8	9.0	2.5	SO-8
Si4308DY	30	12	0.0100		0.0110			40.0	10.0	8.8	0.8	0.8	13.5	3.0	SO-14
Si4308DY	30	20	0.0120		0.0180		20.0	11.5	3.0	4.5	1.5	0.8	9.6	2.0	SO-14
Si4356DY	30	12	0.0060		0.0075			30.0	7.2	6.7	2.0	0.6	17.0	3.0	SO-8
Si4362DY	30	12	0.0045		0.0055			40.0	12.8	7.7	1.3	0.6	20.0	3.5	SO-8
Si4364DY	30	16	0.0045		0.0055			48.0	16.0	11.0	1.1	0.8	20.0	3.5	SO-8
Si4366DY	30	12	0.0048		0.0055			48.0	17.0	10.0	1.3	1.3	20.0	3.5	SO-8
Si4376DY	30	20	0.02		0.0275		20.0	9.0	3.8	3.1	1.3	1.0	7.5	2.0	SO-8
Si4376DY	30	12	0.019		0.023		28.0	12.5	4.0	3.2	1.3	0.8	7.5	2.0	SO-8
Si4404DY	30	20	0.0040		0.0080		75.0	36.0	15.0	12.0		1.0	23.0	3.5	SO-8
Si4406DY	30	20	0.0045		0.0055			34.0	15.0	10.0	1.3	1.0	20.0	3.5	SO-8
Si4408DY	20	20	0.0045		0.0068			21.0	8.9	6.4	1.4	1.0	21.0	3.5	SO-8
Si4412ADY	30	20	0.0240		0.0350		16.0	6.5	3.0	1.5		1.0	8.0	2.5	SO-8
Si4426DY	20	12			0.0250	0.0350		25.0	6.5	4.0		0.6	8.5	2.5	SO-8
Si4433DY	-20	8			0.1100	0.1600		4.4	1.4	0.7		0.5	3.9	2.5	SO-8
Si4442DY	30	12	0.0045		0.0050	0.0075	80.0	36.0	8.0	10.5		0.6	22.0	3.5	SO-8
Si4450DY	60	20	0.0240	0.0300	0.0300		31.0		7.7	8.3		2.0	7.5	2.5	SO-8
Si4466DY	20	12			0.0090	0.0130		50.0	13.0	9.0		0.6	13.2	2.5	SO-8
Si4470EY	60	20	0.0110	0.0130	0.0130		46.0	25.0	11.5	11.5		2.0	12.7	3.8	SO-8
Si4480EY	80	20	0.0350	0.0400	0.0400		30.0	15.0	9.0	5.6		2.0	6.2	3.0	SO-8
Si4482DY	100	20	0.0600	0.0800	0.0800		30.0	14.0	7.5	7.0		2.0	4.6	2.5	SO-8
Si4484EY	100	20	0.0340	0.0400	0.0400		24.0	14.0	7.6	5.4		2.0	6.9	3.8	SO-8
Si4486EY	100	20	0.0250	0.0280	0.0280		36.0	20.0	10.0	8.6		2.0	7.9	3.8	SO-8
Si4488DY	150	20	0.0500				30.0	16.5	8.5	8.5		2.0	5.0	3.1	SO-8
Si4490DY	200	20	0.0800	0.0900	0.0900		34.0	20.0	7.5	12.0		2.0	4.0	3.1	SO-8
Si4496DY	100	20	0.0250	0.0310	0.0310		29.0	6.5	9.9	10.3	1.2	2.0	7.7	3.1	SO-8
Si4724CY	30				0.0375								5.1	1.2	SO-16
Si4724CY	30				0.029								6.5	1.2	SO-16
Si4732CY	30	12			0.0080		46	3.5						4.0	SO-16
Si4732CY	30	20			0.0240		10	7.0						4.0	SO-16
Si4736DY	30	12	0.0100		0.0110			37.0	10.0	8.8	0.8	1.0	13.0	3.1	SO-8
Si4738CY	20				0.009		19								SO-16
Si4738CY	20				0.006		38								SO-16
Si4800DY	30	25	0.0180		0.0330		8.7	15.0	2.3	4.2		0.8	9.0	2.5	SO-8
Si4804DY	30	20	0.0220		0.0300		13.0	7.0	2.0	2.7	1.3	0.8	7.5	2.0	SO-8
Si4808DY	30	20	0.0220		0.0300		13.0	7.0	2.0	2.7	1.3	0.8	7.5	2.0	SO-8
Si4810DY	30	20	0.0130		0.0200		36.0	20.0	8.0	7.0		1.0	10.0	2.5	SO-8



Alphanumeric Index (cont'd.)															
Part Number	V <sub>DS</sub> (V)	V <sub>GS</sub> (V)	r <sub>DS(on)</sub> Ω				Q <sub>g</sub> (nC)		Q <sub>GS</sub> (nC)	Q <sub>GD</sub> (nC)	R <sub>g</sub> Typ (Ω)	V <sub>th</sub> (V)	I <sub>D</sub> (A)	P <sub>D</sub> (W)	Package
			V <sub>GS</sub> = 10V	V <sub>GS</sub> = 6V	V <sub>GS</sub> = 4.5V	V <sub>GS</sub> = 2.5V	V <sub>GS</sub> = 10V	V <sub>GS</sub> = 4.5V							
Si4812DY	30	20	0.0180		0.0280		27.5	16.0	6.0	6.0		1.0	9.0	2.5	SO-8
Si4814DY	30	20	0.0200		0.0265		19.0	9.7	2.6	3.8	1.8	0.8	7.4	2.0	SO-8
Si4814DY	30	20	0.0210		0.0325		12.0	6.5	1.5	2.7	1.6	0.8	7.0	1.9	SO-8
Si4816DY	30	20	0.0220		0.0300		14.0	8.0	1.8	3.2		0.8	6.3	1.4	SO-8
Si4816DY	30	20	0.0130		0.0185		29.0	15.0	5.3	4.6		1.0	10.0	2.4	SO-8
Si4818DY	30	20	0.0220		0.0300		14.0	8.0	1.8	3.2		0.8	6.3	1.4	SO-8
Si4818DY	30	20	0.0155		0.0205		29.0	15.0	5.3	4.6		1.0	9.5	2.4	SO-8
Si4820DY	30	20	0.0130		0.0200		37.0	20.0	8.0	7.0		1.0	10.0	2.5	SO-8
Si4824DY	30	20	0.0175		0.0270		31.0	17.5	7.5	6.5		1.0	9.0	2.3	SO-8
Si4824DY	30	20	0.0400		0.0650		11.0	6.5	3.0	2.5		1.0	4.7	1.4	SO-8
Si4826DY	30	20	0.0150		0.0200		29.0	15.0	5.3	4.6		1.0	9.5	2.4	SO-8
Si4826DY	30	20	0.0220		0.0300		14.0	8.0	1.8	3.2		0.8	6.3	1.4	SO-8
Si4830ADY	30	12	0.0220		0.0290			5.0	2.0	1.5		1.2			SO-8
Si4830DY	30	20	0.0220		0.0300		13.0	7.5	2.0	2.7	1.3	0.8	7.5	2.0	SO-8
Si4832DY	30	20	0.0180		0.0280		27.5	16.0	6.0	6.0		1.0	9.0	2.5	SO-8
Si4834DY	30	20	0.0220		0.0300		13.0	7.5	2.0	2.7	1.3	0.8	7.5	2.0	SO-8
Si4835DY	-30	25	0.0190		0.0330		37.0	21.0	6.5	8.0		1.0	8.0	2.5	SO-8
Si4836DY	12	8			0.0030	0.0040		56.0	8.0	10.5	1.6	0.4	25.0	3.5	SO-8
Si4837DY	-30	20	0.0200		0.0300		40.0	22.0	9.0	6.6		1.0	8.3	2.5	SO-8
Si4838DY	12	8			0.0030	0.0040		40.0	6.7	9.2		0.6	25.0	3.5	SO-8
Si4840DY	40	20	0.0090		0.0120		35.0	18.5	6.0	7.5		1.0	14.0	3.1	SO-8
Si4842DY	30	20	0.0045		0.0060		55.0	25.0	6.7	9.7		1.0	23.0	3.5	SO-8
Si4848DY	150	20	0.0850	0.0950	0.0950		17.0	10.0	3.2	6.0		2.0	3.7	3.0	SO-8
Si4850EY	60	20	0.0220		0.0310		18.0	9.5	3.4	5.3		1.0	8.5	3.3	SO-8
Si4852DY	30	20	0.0120		0.0175		41.0	23.0	8.6	7.2		1.0	11.0	2.5	SO-8
Si4854DY	30	12	0.0260		0.0300	0.0410	20.0	9.0	2.1	2.6		0.6	6.9	2.0	SO-8
Si4856DY	30	20	0.0060		0.0085			21.0	8.0	7.2	1.5	1.0	17.0	3.0	SO-8
Si4858DY	30	20	0.0053		0.0070		65.0	30.5	13.5	9.5	1.4	1.0	20.0	3.5	SO-8
Si4860DY	30	20	0.0080		0.0110			13.0	5.0	4.0	1.7	1.0	16.0	3.5	SO-8
Si4862DY	16	8			0.0033	0.0055		48.0	11.8	8.9	1.3	1.2	25.0	3.5	SO-8
Si4864DY	20	8			0.0035	0.0047		47.0	10.0	13.4	1.5	0.6	25.0	3.5	SO-8
Si4866DY	12	8			0.0055	0.0080		21.0	4.6	3.5	2.3	0.6	17.0	3.0	SO-8
Si4876DY	20	12			0.0050	0.0075	55.0	55.0	13.0	11.0		0.6	21.0	3.0	SO-8
Si4884DY	30	20	0.0100		0.0160		30.0	15.3	5.8	4.8	2.2	1.0	12.0	3.0	SO-8
Si4888DY	30	20	0.0070		0.0100		32.0	16.3	4.0	5.9		0.8	16.0	3.5	SO-8
Si4892DY	30	20	0.0120		0.0200		16.0	8.7	2.4	3.5	1.0	0.8	12.4	3.1	SO-8
Si4894DY	30	20	0.0120		0.0180		20.0	11.0	3.0	4.5		0.8	12.5	3.0	SO-8
Si4896DY	80	20	0.0165	0.0220	0.0220		34.0	21.0	7.5	11.0		2.0	9.5	3.1	SO-8
Si4924DY	30	20	0.0100		0.0140		43.0	25.5	4.5	11.5		0.8	11.5	2.4	SO-8
Si4924DY	30	20	0.0220		0.0300		14.0	8.0	1.8	3.2		0.8	6.3	1.4	SO-8
Si4926DY	30	20	0.0125		0.0170		30.0	18.0	3.6	7.8		0.8	10.5	2.4	SO-8
Si4926DY	30	20	0.0220		0.0300		14.0	8.0	1.8	3.2		0.8	6.3	1.4	SO-8
Si4942DY	40	20	0.0210		0.0280		21.0	11.0	3.3	5.8	1.1	1.0	7.4	2.1	SO-8
Si4946EY	60	20	0.0550		0.0750		19.0	9.0	4.0	3.0		1.0	4.5	2.0	SO-8
Si4980DY	80	20	0.0750	0.0950	0.0950		15.0		3.2	4.0		2.0	3.7	2.0	SO-8
Si4982DY	100	20	0.1500	0.1800	0.1800		15.0	7.0	4.0	2.7		2.0	2.6	2.0	SO-8
Si5515DC	-20	8			0.1310	0.1850		3.1				0.6	2.9	2.1	1206-8 ChipFET
Si5515DC	20	8			0.0760	0.1030		4.3				0.6	4.2	2.1	1206-8 ChipFET
Si6410DQ	30	20	0.0140		0.0210		40.0	22.5	9.0	7.0		1.0	7.8	1.5	TSSOP-8
Si6434DQ	30	20	0.0280		0.0420		18.0	9.0	3.3	2.6		1.0	5.6	1.5	TSSOP-8
Si6466DQ	20	12			0.0140	0.0210		34.0	8.1	6.7		0.6	7.8	1.5	TSSOP-8
Si6802DQ	20	12			0.0750			4.5	1.0	0.7		0.6	3.3	1.5	TSSOP-8
Si6820DQ	20	20			0.1600			2.1	0.4	0.3		0.6	1.9	1.2	TSSOP-8
Si7358DP	30	20	0.0053		0.0070		65.0	30.5	13.5	9.5	1.4	1.0	23.0	5.4	PowerPAK SO-8
Si7370DP	60	20	0.0110	0.0130			46.0	24.0	11.5	11.5	0.9	2.0	15.8	5.2	PowerPAK SO-8
Si7388DP	30	20	0.007		0.010		31	16.3	4	5.9		0.8	19	5	PowerPAK SO-8
Si7404DN	30	12	0.0130		0.0150	0.0220	47.0	20.0	5.8	7.1		0.6	13.3	3.8	PowerPAK 1212-8



Alphanumeric Index (cont'd.)															
Part Number	V <sub>DS</sub> (V)	V <sub>GS</sub> (V)	r <sub>DS(on)</sub> Ω				Q <sub>g</sub> (nC)		Q <sub>GS</sub> (nC)	Q <sub>GD</sub> (nC)	R <sub>g</sub> Typ (Ω)	V <sub>th</sub> (V)	I <sub>D</sub> (A)	P <sub>D</sub> (W)	Package
			V <sub>GS</sub> = 10V	V <sub>GS</sub> = 6V	V <sub>GS</sub> = 4.5V	V <sub>GS</sub> = 2.5V	V <sub>GS</sub> = 10V	V <sub>GS</sub> = 4.5V							
Si7414DN	60	20	0.0250		0.0360		16.0	8.0	2.7	4.4	1.0	1.0	8.7	3.8	PowerPAK 1212-8
Si7415DN	-60	20	0.0650		0.1100		15.0	7.5	4.0	3.2		1.0	5.7	3.8	PowerPAK 1212-8
Si7440DP	30	20	0.0065		0.0080		10.0	29.0	10.5		1.4	1.0	21.0	5.4	PowerPAK SO-8
Si7445DP	-20	8			0.0077	0.0094		92.0	19.0	16.5	2.0	0.5	19.0	5.4	PowerPAK SO-8
Si7446DP	30	20	0.0075		0.0100		76.0	36.0	14.0	12.0	2.4	1.0	19.0	5.2	PowerPAK SO-8
Si7448DP	20	12			0.0065	0.0090		38.0	8.0	8.5	0.9	0.6	22.0	5.2	PowerPAK SO-8
Si7450DP	200	20	0.0800	0.0900	0.0900		34.0	20.0	7.5	12.0		2.0	5.3	5.2	PowerPAK SO-8
Si7454DP	100	20	0.0340	0.0400	0.0400		24.0	14.0	7.6	5.4		2.0	7.8	4.8	PowerPAK SO-8
Si7456DP	100	20	0.0250	0.0280	0.0280		36.0	20.0	10.0	8.6	1.3	2.0	9.3	5.2	PowerPAK SO-8
Si7458DP	20	12			0.0045	0.0075		38.0	8.0	8.5		0.6	22.0	5.2	PowerPAK SO-8
Si7540DP	12	8			0.0210	0.0260						0.7			PowerPAK SO-8
Si7540DP	-12	8			0.0340	0.0470						0.7			PowerPAK SO-8
Si7806DN	30	20	0.0110		0.0175		19.0	8.5	3.6	3.0	2.0	1.0	14.4	3.8	PowerPAK 1212-8
Si7810DN	100	20	0.0620	0.0840	0.0840		13.0	7.8	3.0	4.6		2.0	5.4	3.8	PowerPAK 1212-8
Si7840DP	30	20	0.0095		0.0140		29.0	15.5	3.8	6.0	0.8	1.0	18.0	5.0	PowerPAK SO-8
Si7842DP	30	20	0.0220		0.0300		13.0	7.0	2.0	2.7	1.2	0.8	10.0	3.5	PowerPAK SO-8
Si7844DP	30	20	0.0220		0.0300		13.0	7.0	2.0	2.7	1.2	0.8	10.0	3.5	PowerPAK SO-8
Si7846DP	150	20	0.0500				30.0	18.0	8.5	8.5		2.0	6.7	5.2	PowerPAK SO-8
Si7848DP	40	20	0.0090		0.0120		35.0	18.5	6.0	7.5	0.8	1.0	17.0	5.0	PowerPAK SO-8
Si7850DP	60	20	0.0220		0.0310		18.0	9.5	3.4	5.3	1.4	1.0	10.3	4.5	PowerPAK SO-8
Si7852DP	80	20	0.0165	0.0220	0.0220		34.0	22.0	7.5	11.0	0.9	2.0	12.5	5.2	PowerPAK SO-8
Si7856DP	30	20	0.0045		0.0055		34.0	15.0	10.0	1.3	1.0	25.0	5.4	5.4	PowerPAK SO-8
Si7858DP	12	8			0.0030	0.0040					1.0	0.6			PowerPAK SO-8
Si7860DP	30	20	0.0080		0.0110		13.0	5.0	4.0	1.7	1.0	18.0	5.0	5.0	PowerPAK SO-8
Si7862DP	16	8			0.0033	0.0055		48.0	11.8	8.9	1.3	0.6	29.0	5.4	PowerPAK SO-8
Si7864DP	20	8			0.0035	0.0047		47.0	10.0	13.4	1.5	0.6	29.0	5.4	PowerPAK SO-8
Si7866DP	20	20	0.0025		0.0033		40.0	15.0	11.0	1.2	0.8	29.0	5.4	5.4	PowerPAK SO-8
Si7868DP	20	16	0.0023		0.0028		50.0	12.0	11.0	1.2	0.6	29.0	5.4	5.4	PowerPAK SO-8
Si7880DP	30	20	0.0030		0.0043		88.0	40.5	18.0	10.5	1.2	1.0	29.0	5.4	PowerPAK SO-8
Si7882DP	12	8			0.0055	0.0080		21.0	4.6	3.5		0.6	22.0	5.0	PowerPAK SO-8
Si7884DP	40	20	0.0070		0.0095		35.0	18.5	6.0	7.5	0.8	1.0	20.0	5.2	PowerPAK SO-8
Si7886DP	30	12	0.0045		0.0055		42.0	12.8	7.7	1.3	0.6	25.0	5.4	5.4	PowerPAK SO-8
Si7888DP	30	20	0.0120		0.0200		16.0	8.7	2.4	3.5	1.0	0.8	15.7	5.0	PowerPAK SO-8



Alphanumeric Index (cont'd.)															
Part Number	V <sub>DS</sub> (V)	V <sub>GS</sub> (V)	r <sub>DS(on)</sub> Ω				Q <sub>g</sub> (nC)		Q <sub>GS</sub> (nC)	Q <sub>GD</sub> (nC)	R <sub>g</sub> Typ (Ω)	V <sub>th</sub> (V)	I <sub>D</sub> (A)	P <sub>D</sub> (W)	Package
			V <sub>GS</sub> = 10V	V <sub>GS</sub> = 6V	V <sub>GS</sub> = 4.5V	V <sub>GS</sub> = 2.5V	V <sub>GS</sub> = 10V	V <sub>GS</sub> = 4.5V							
Si7892DP	30	20	0.0045		0.0060		55.0	25.0	6.7	9.7	1.9	1.0	25.0	5.4	PowerPAK SO-8
Si7894DP	30	12	0.0045		0.0055			48.0	17.0	10.0	1.3	0.6	25.0	5.4	PowerPAK SO-8
Si7898DP	150	20	0.0850	0.0950			17.0	10.0	3.2	6.0	0.9	2.0	4.8	5.0	PowerPAK SO-8
Si7922DN	100	20	0.1700	0.2060	0.2060							2.0			PowerPAK 1212-8
Si7940DP	12	8			0.0170	0.0250		11.5	3.2	2.5		0.6	11.8	3.5	PowerPAK SO-8
Si9420DY	200	20	1.0000				8.6	5.0	1.5	3.2		2.0	1.0	2.5	SO-8
Si9422DY	200	20	0.4200				13.0		4.5	3.5		2.0	1.7	2.5	SO-8
Si9428DY	20	8			0.0300	0.0400		21.0	6.5	2.9		0.6	6.0	2.5	SO-8
SUB40N06-25L	60	20	0.0220		0.0250		40.0	18.0	9.0	10.0		1.0	40.0	90.0	D <sup>2</sup> PAK (TO-263)
SUB70N03-09BP	30	20	0.0090		0.0130		26.0	15.5	5.0	6.0		0.8	70.0	93.0	D <sup>2</sup> PAK (TO-263)
SUB75N06-07L	60	20	0.0070		0.0080		75.0	50.0	18.0	27.0		1.0	75.0	250.0	D <sup>2</sup> PAK (TO-263)
SUB75N06-08	60	20	0.0080				85.0		28.0	26.0		2.0	75.0	250.0	D <sup>2</sup> PAK (TO-263)
SUB85N02-03	20	8			0.0030	0.0034		140.0	18.0	24.0		0.5	85.0	250.0	D <sup>2</sup> PAK (TO-263)
SUB85N02-06	20	12			0.0060	0.0090	135.0	65.0	13.0	14.0		0.6	85.0	120.0	D <sup>2</sup> PAK (TO-263)
SUB85N03-04P	30	20	0.0040		0.0070		71.0	35.0	15.0	16.0		1.0	85.0	166.0	D <sup>2</sup> PAK (TO-263)
SUB85N03-07P	30	20	0.0070		0.0100		60.0	26.0	13.0	10.0		1.0	85.0	107.0	D <sup>2</sup> PAK (TO-263)
SUB85N06-05	60	20	0.0050		0.0070		155.0	70.0	28.0	44.0		1.0	85.0	250.0	D <sup>2</sup> PAK (TO-263)
SUB85N10-10	100	20	0.0100		0.0120		105.0	55.0	17.0	23.0		1.0	85.0	250.0	D <sup>2</sup> PAK (TO-263)
SUD15N15-95	150	20	0.0950	0.1000	0.1000								15.0	62.0	DPAK (TO-252)
SUD19N20-90	200	20	0.0900	0.1050	0.1050		34.0	7.5	8.0	12.0		2.0	19.0	100.0	DPAK (TO-252)
SUD25N15-52	150	20	0.0520	0.0600	0.0600		33.0	7.5	9.0	12.0		2.0	25.0	100.0	DPAK (TO-252)
SUD30N04-10	40	20	0.0100		0.0140		50.0	23.0	9.0	11.0		1.0	30.0	97.0	DPAK (TO-252)
SUD40N02-08	20	12			0.0085	0.0140	54.0	26.0	5.0	7.0		0.6	40.0	71.0	DPAK (TO-252)
SUD40N06-25L	60	20	0.0220		0.0250		40.0	18.0	9.0	10.0		1.0	20.0	75.0	DPAK (TO-252)
SUD40N08-16	80	20	0.0160				42.0	22.0	7.0	13.0		2.0	40.0	100.0	DPAK (TO-252)
SUD40N10-25	100	20	0.0250		0.0280		40.0		11.0	9.0		1.0	40.0	33.0	DPAK (TO-252)
SUD50N02-06	20	12			0.0060	0.0090		65.0	13.0	14.0		0.6	30.0	100.0	DPAK (TO-252)
SUD50N03-07	30	20	0.0070		0.0100		70.0	35.0	16.0	10.0		1.0	20.0	83.0	DPAK (TO-252)
SUD50N03-07AP	30	20	0.0070		0.0100		60.0	28.0	12.0	10.0	1.8	1.0	25.0	88.0	DPAK (TO-252)
SUD50N03-06P	30	20	0.0065		0.0095		48.0	22.0	10.0	7.5	1.9	1.0	25.0	88.0	DPAK (TO-252)
SUD50N03-09P	30	20	0.0095		0.0140		31.0	13.5	7.5	5.0	1.5	1.0	21.0	65.2	DPAK (TO-252)
SUD50N03-10BP	30	20	0.0100		0.0140		27.0	15.5	5.0	6.0		0.8	20.0	71.0	DPAK (TO-252)
SUD50N03-10CP	30	20	0.0100		0.0120		38.0	13.0	4.5	4.0	1.7	1.0	15.0	71.0	DPAK (TO-252)
SUM110N10-09	100	20	0.0095				110.0	55.0	24.0	24.0		2.0	110.0	437.5	D <sup>2</sup> PAK (TO-263)

Alphanumeric Index (cont'd.)															
Part Number	V <sub>DS</sub> (V)	V <sub>GS</sub> (V)	r <sub>DS(on)</sub> Ω				Q <sub>g</sub> (nC)		Q <sub>GS</sub> (nC)	Q <sub>GD</sub> (nC)	R <sub>g</sub> Typ (Ω)	V <sub>th</sub> (V)	I <sub>D</sub> (A)	P <sub>D</sub> (W)	Package
			V <sub>GS</sub> = 10V	V <sub>GS</sub> = 6V	V <sub>GS</sub> = 4.5V	V <sub>GS</sub> = 2.5V	V <sub>GS</sub> = 10V	V <sub>GS</sub> = 4.5V							
SUM65N20-30	200	20	0.0300				90.0	17.0	23.0	34.0		2.0	65.0	375.0	D <sup>2</sup> PAK (TO-263)
SUM85N03-06P	30	20	0.0060		0.0090		48.0	22.0	10.0	7.5	1.9	1.0	85.0	100.0	D <sup>2</sup> PAK (TO-263)
SUM85N03-08P	30	20	0.0075		0.0105		37.5	13.0	4.5	4.0	1.9	1.0	85.0	100.0	D <sup>2</sup> PAK (TO-263)
SUM85N15-19	150	20	0.0190				76.0	17.0	21.0	26.0		2.0	85.0	375.0	D <sup>2</sup> PAK (TO-263)
SUP18N15-95	150	20	0.0950	0.1000	0.1000								18.0	88.0	TO-220
SUP70N03-09BP	30	20	0.0090		0.0130		26.0	15.5	5.0	6.0		0.8	70.0	93.0	TO-220
SUP85N02-03	20	8			0.0030	0.0034		140.0	18.0	24.0		0.5	85.0	250.0	TO-220
SUP85N03-04P	30	20	0.0040		0.0070		71.0	35.0	15.0	16.0		1.0	85.0	166.0	TO-220
SUP85N03-07P	30	20	0.0070		0.0100		60.0	26.0	13.0	10.0		1.0	85.0	107.0	TO-220
SUP85N10-10	100	20	0.0100		0.0120		105.0	55.0	17.0	23.0		1.0	85.0	250.0	TO-220
SUU15N15-95	150	20	0.0950	0.1000	0.1000		20.0	5.0	5.5	7.0		2.0	15.0	62.0	TO-251
SUY50N03-10CP	30	20	0.0100		0.0120		38.0	13.0	4.5	4.0	1.7	1.0	15.0	71.0	TO-251
TN0201T	20	20	0.7500		1.0000		1.4	0.8	0.3	0.2		1.0	0.4	0.4	SOT-23



**PWM Converters and Controllers, and MOSFET Drivers**

Part Number	Package	Topology	Input Voltage (V)	Mode	Maximum Oscillator Frequency (MHz)	Reference Voltage (V)	Maximum Supply Current (mA)
<b>Distributed Power</b>							
Si9100*	PDIP-14 PLCC-20	Buck, Flyback, Forward	10 - 70	Current	1	4	1
Si9102*	PDIP-14 PLCC-20	Buck, Flyback, Forward	10 - 120	Current	1	4	1
Si9104*	SO-16WB	Buck, Flyback, Forward	10 - 120	Current	1	4	1
Si9105*	SO-16WB PDIP-14 PLCC-20	Buck, Flyback, Forward	10 - 120	Current	1	4	0.5
Si9108	SO-16WB PDIP-14 PLCC-20	Buck, Flyback, Forward	10 - 120	Current	1	4	0.5
Si9110	SO-14 PDIP-14	Buck, Flyback, Forward	10 - 120	Current	1	4	1
Si9111	SO-14 PDIP-14	Buck, Flyback, Forward	10 - 120	Current	1	4	1
Si9112	SO-14 PDIP-14	Buck, Flyback, Forward	10 - 120	Current	1	4	1
Si9113	SO-14	Buck, Flyback, Forward	23 - 200	Current	0.5	1.3	1.4
Si9114A	SO-14 PDIP-14	Buck, Flyback, Forward	15 - 200	Current	1	4	3
Si9117*	SO-16	Buck, Flyback, Forward	15 - 200	Current	1	4	4.5
Si9118	SO-16	Boost, Flyback, Forward	10 - 200	Current	1	4	2.5
Si9119	SO-16	Boost, Flyback, Forward	10 - 200	Current	1	4	2.5
Si9121-5*	SO-8	Buck/Boost Converter	-10 to -60	Current	0.11	1.25	1.5
Si9121-3.3*	SO-8	Buck/Boost Converter	-10 to -60	Current	0.11	1.25	1.5
Si9138	SSOP-28	Triple outut, individual On/Off Control Power Supply Controller	5.5 - 30	Current	0.33	3.3	1.8
<b>Offline</b>							
Si9120	SO-16 PDIP-16	Buck, Flyback, Forward	15 - 450	Current	1	4	1.5
<b>Computer Point-of-Use</b>							
Si9140	SO-16	Buck	2.7 - 8	Voltage	2	1.5	1
Si9142	SO-20	Buck	4.75 - 13.2	Voltage	1	1.3	1.2
Si9143	SSOP-24	Buck, ISHARE	4.75 - 13.2	Voltage	1	1.3	1.2
Si9145	SO-16 TSSOP-16	Buck, Boost, Flyback, Forward	2.7 - 8	Voltage	2	1.5	1.4
<b>Portable Computer</b>							
Si786	SSOP-28	Dual Synchronous Buck	5.5 - 30	Current	0.3	3.3	1.6
Si9130	SSOP-28	Dual Synchronous Buck	5.5 - 30	Current	0.3	3.3	1.6
Si9135	SSOP-28	Triple Output, SMBus	5.5 - 30	Current	0.3	3.3	1.8
Si9136	SSOP-28	Triple Output	5.5 - 30	Current	0.3	3.3	1.8
Si9137	SSOP-28	Triple output, sequence selectable controller	5.5 - 30	Current	0.33	3.3	1.8

<b>Mosfet Drivers</b>							
Part Number	Function	Supply Voltage	Output Drive Capacity	Input Drive Requirements	Features	Package	Protection
Si9910	High Voltage Mosfet Driver	11 - 16 for Driver	Drives 1 N-Ch. MOSFET	12-V Logic	dv/dt, di/dt Control	DIP-8, SO-8	Short Circuit, Under Voltage
Si9912	Half Bridge Mosfet driver	4.5 - 30V	Drives 2 N-Ch. MOSFET	5 V , TTL/CMOS	Shutdown Quiescent current	SO-8	Undervoltage. Shoot Through
Si9913	Half Bridge Mosfet driver	4.5 - 30V	Drives 2 N-Ch. MOSFET	5 V , TTL/CMOS	Synchronous switch enable	SO-8	Undervoltage. Shoot Through

\*Converters, with integrated MOSFET